

Growth and Coalescence Studies of $(11\bar{2}2)$ Oriented GaN on Pre-Structured Sapphire Substrates Using Marker Layers

Marian Caliebe

In this article¹, the growth and coalescence of semipolar $(11\bar{2}2)$ oriented GaN layers, deposited on pre-structured r-plane sapphire substrates, is studied with the help of Si-doped marker layers. It has been found to be very important to adjust the shape of the initial GaN stripes by varying the growth temperature to obtain not only a smooth surface, but also a low density of basal plane stacking faults (BSFs) and threading dislocations (TDs) on the wafer surface. With the help of transmission electron microscopy (TEM) and cathodoluminescence measurements (CL), we can conclude that during growth, we need to achieve a compromise between low BSF density, low TD density, and perfect coalescence with smooth surface, free of fissures and other growth artifacts.

1. Introduction

A promising approach for the production of green and yellow GaN-based light-emitting diodes (LEDs) is the usage of semipolar substrates. Compared to commercial c-oriented devices, these substrates have a reduced piezo-electric field in the quantum wells. Thus, the influence of the quantum-confined Stark effect can be reduced, which is expected to result in higher efficiency of the recombination of carriers in the quantum wells [2–6].

The samples studied in this article are produced based on a method first demonstrated by Okada *et al.* [7]. We use 2" r-plane sapphire wafers for hetero-epitaxy. These substrates are patterned with trenches parallel to the a-direction of the sapphire. A special property of these trenches is that one of the side-facets is c-plane-like. Under appropriate GaN growth conditions, the selectivity is large enough that growth mainly takes place on these c-plane-like facets, resulting in GaN stripes that coalesce after some time into a closed layer with the desired $(11\bar{2}2)$ surface. Compared to epitaxy on planar m-oriented sapphire, a much better crystal quality can be achieved [8].

While Okada *et al.* [7] focused on this growth method itself and on growth selectivity on the different sapphire crystal planes, Kurisu *et al.* [9] studied the variation of the shape of the uncoalesced GaN stripes by varying the temperature and V/III ratio and selected the optimum parameters merely by judging the growth selectivity, the shape of the GaN stripes and their surface morphology (before coalescence). However, we focus our studies on the influence of the shape on the fully grown sample by having a closer look on the

¹For the full version of this article see [1].

coalescence behavior and study its impact on defects in the final structure with the help of marker layers. In both publications [7,9], dislocations and stacking faults were already detected by TEM, but their development and propagation has not yet been studied in detail.

The marker layers in this article are produced by doping with Si and can be observed as a contrast caused by changed electrical conductivity in scanning electron microscopy (SEM) [10]. They give direct insight into the growth evolution. It is easily possible to recognize at each point the shape of the growth front. Also, we can immediately observe, how a change of the growth conditions influences the local growth behavior. Moreover, it is possible to correlate the shape found in SEM micrographs on the cross-section with transmission electron microscopy (TEM) images, to understand the propagation of threading dislocations. Comparing samples with and without marker layers, we observed that the influence of the marker layers on the crystal quality is negligible.

2. Experimental

2.1 Sample preparation

The metal organic vapor phase epitaxy (MOVPE) growth experiments are conducted on (1 $\bar{1}$ 02)-oriented sapphire substrates, which are structured in the following way: First, a pattern of resist stripes with a period of 6 μm and an aspect ratio of 1:1 is prepared by common photolithography. Then, trenches are etched by reactive-ion etching (RIE) using the gases Ar, BCl_3 , and Cl_2 . Afterwards, the remaining resist is removed in O_2 plasma. Finally, the sapphire is cleaned wet-chemically with KOH and piranha solution ($\text{H}_2\text{SO}_4:\text{H}_2\text{O}_2$).

2.2 MOVPE growth conditions

The sapphire wafers are overgrown in a commercial Aixtron-200/4 RF-S HT reactor using the precursors TMGa, NH_3 , TMAI, and SiH_4 . The indicated growth temperatures are the reactor temperatures measured on the backside of the susceptor which may differ from the real wafer temperature. The sample structure is sketched in Fig. 1 and given in Table 1. First, an intentionally doped AlN:O nucleation layer with an oxygen content of approximately 10%, similar as in our standard c-plane growth [11, 12], is deposited. Then, a GaN buffer layer (layer I) is grown at 1080 $^\circ\text{C}$, a TMGa flow of $f(\text{TMGa}) = 102 \mu\text{mol}/\text{min}$ with a V/III ratio of 870, and a reactor pressure of 150 hPa. After 3.5 min, the reactor temperature is slowly ramped to 1000 $^\circ\text{C}$. After growth of approximately 0.5 μm on the c-facet of the sapphire trench, an in situ deposited SiN_x interlayer (layer II) is incorporated for defect reduction using SiH_4 [13]. Then, GaN growth continues for further 6 min. In the next 50 min, the GaN stripe (layer III) is formed. In layer III, 5 marker layers are incorporated by doping for 2 min with SiH_4 in a period of 10 min with an estimated resulting n -carrier density of $\sim 5 \cdot 10^{19} \text{cm}^{-3}$. Then, the reactor temperature is set to 970 $^\circ\text{C}$ for 40 min (4 marker layers) to deposit a GaN interlayer (layer IV). Its purpose is discussed in [1]. Finally, in layer V, the reactor parameters are set to

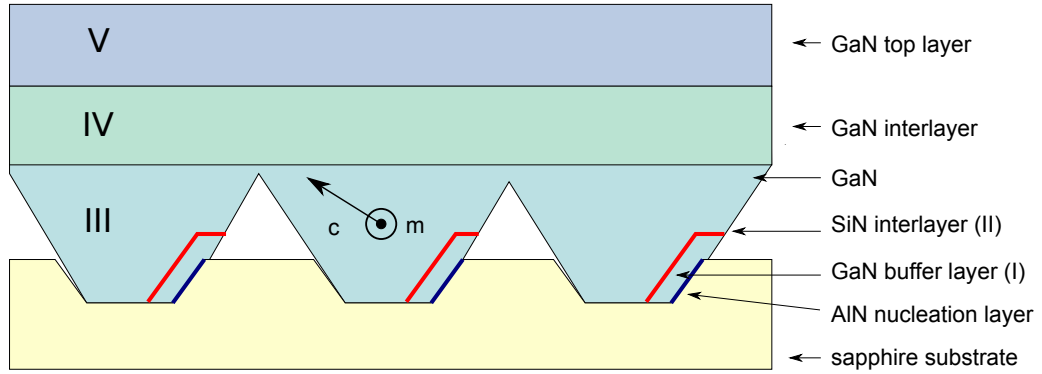


Fig. 1: Sketch of the layer sequence of samples A, B, and C.

Table 1: Layer sequence of the samples studied in Sect. 3.1. The marker layers are deposited in a period of 10 min.

Layer	Layer #	Growth conditions	Sample #	Marker layers
GaN top layer	V	1041 °C, V/III = 140, $f(\text{TMGa}) = 156 \mu\text{mol}/\text{min}$		3
GaN interlayer	IV	970 °C		4
GaN stripe	III	6 min, ramp to $x = \begin{cases} 950^\circ\text{C} \\ 1000^\circ\text{C} \\ 1050^\circ\text{C} \end{cases}$	A B C	5
SiN _x interlayer	II	1000 °C		-
GaN buffer layer	I	1080 °C, ramp to 1000 °C		-

$T = 1041^\circ\text{C}$, $V/\text{III} = 140$, and $f(\text{TMGa}) = 156 \mu\text{mol}/\text{min}$ (resulting in a higher growth rate), since this has been found to be the optimum conditions after coalescence [14]. Under these conditions, 3 marker layers are deposited.

In this experiment, the growth temperature before coalescence (layer III) is varied between 950°C and 1050°C (Table 1) to study its influence on the resulting layer quality. Besides SEM and TEM studies, CL is used to investigate the distribution of BSFs and dark spots on the wafer surface, which allows inference to the distribution and density of TDs. The ratio of the BSF I_1 at 3.41 eV towards the donor bound exciton (D^0X) peak in photoluminescence (PL) is a qualitative measure of the amount of BSFs on the wafer surface. Further, the full width at half maximum (FWHM) of high resolution X-ray diffraction (HRXRD) rocking curves allows inference to the crystal quality. Atomic force microscopy (AFM) is used to determine the surface texture and roughness.

3. Results and Discussion

3.1 Shape of initial GaN stripes

In Fig. 2 (first row), SEM micrographs of the samples' cross-sections are presented, which show the marker layers. In TEM, (Fig. 2, second row), the marker layers are not visible. The black lines in these images are threading dislocations.

By the course of the marker layers, it can be observed that at 950 °C (sample A), the shape of the initial GaN stripes is only formed by $\{11\bar{2}2\}$ planes. By increasing the temperature to 1000 °C (sample B), also (0001) and $(11\bar{2}0)$ planes appear. At 1050 °C (sample C), they become larger than the $(11\bar{2}2)$ surface plane. This behavior has already been observed by Kurisu *et al.* by stopping the growth before coalescence [9].

The initial shape of the GaN stripes has a strong influence on coalescence and the residual layer quality: It is well known that basal plane stacking faults (BSFs) are mainly located in the -c-wing and may be blocked at the coalescence point by a small gap (see e.g. [15–18]). For sample A, no a-plane exists at all. Thus, there is no gap in the coalescence region to block BSFs. They can propagate unhindered to the surface, confirmed by the highest BSF-related peak in PL (Fig. 3) and largest area of BSF induced luminescence in CL (Fig. 2, bottom). Additionally, the neighboring stripe grows in c-direction over the $(11\bar{2}2)$ plane leading to non-planar coalescence. Sometimes this overlap can continue up to the wafer surface resulting in the formation of several 10 μm long surface immersions called “chevrons” that have already been reported by Brunner *et al.* on $(11\bar{2}2)$ GaN samples produced after the same approach [19] and on $(11\bar{2}2)$ GaN grown on m-plane sapphire patterned with a SiO_2 epitaxial lateral overgrowth (ELOG) mask as reported by Zhu *et al.* [20]. While up to now only assumptions about the origin of “chevrons” could be done, we now were able to directly observe their formation (cf. [1]).

The optimum results were achieved for sample B (Fig. 2, center). Here, the surface is already planar shortly after coalescence, which leads to the smoothest surface and narrowest rocking curves in HRXRD (Fig. 4). Also, the small gap at the coalescence region is formed parallel to the a-plane to stop the continuation of BSFs to the surface.

If the sample is grown too hot (sample C), we observe the worst case of coalescence. Now, stripes grow together in a “V”-shape, which is formed by the a- and c-facets of neighboring stripes. However, the BSFs on the c-wing are blocked most effectively leading to the smallest BSF density on the surface (compare PL Fig. 3 and CL Fig. 2, bottom). The “V”-shape often prevents coalescence leading to fissures which propagate to the surface ending in a gap as shown in the SEM cross-section (Fig. 5, left), the SEM bird's eye view (Fig. 5, right) and the AFM image (Fig. 6, right). These fissures strongly decrease the electrical conductivity perpendicular to the stripes. This can be observed e.g. in van der Pauw Hall measurements, manifested in small geometry factors [21].

3.2 TEM investigations

In the TEM images (Fig. 2, second row), it is observed that threading dislocations mainly start on the c-sapphire-GaN interface and propagate in c-direction. TDs bend by 90° to

the a-direction as soon as they hit the $(11\bar{2}2)$ plane (Fig. 2, second row, left). However, if there is a wide c-plane like in sample C, some TDs might never bend and continue propagating in c-direction (Fig. 2, second row, right). A very similar dislocation bending has already been reported on c-oriented samples at 2S-ELO (two-step epitaxial lateral overgrowth) and FACELO (facet-controlled ELO) investigations, respectively [22–24].

Both bent and un-bent dislocations have the chance to propagate to the surface. For good layer quality, the bending should happen as early as possible. This way, the dislocations can be either blocked at the coalescence gap, or are at least cumulated above the coalescence point and not distributed equally over the whole sample surface.

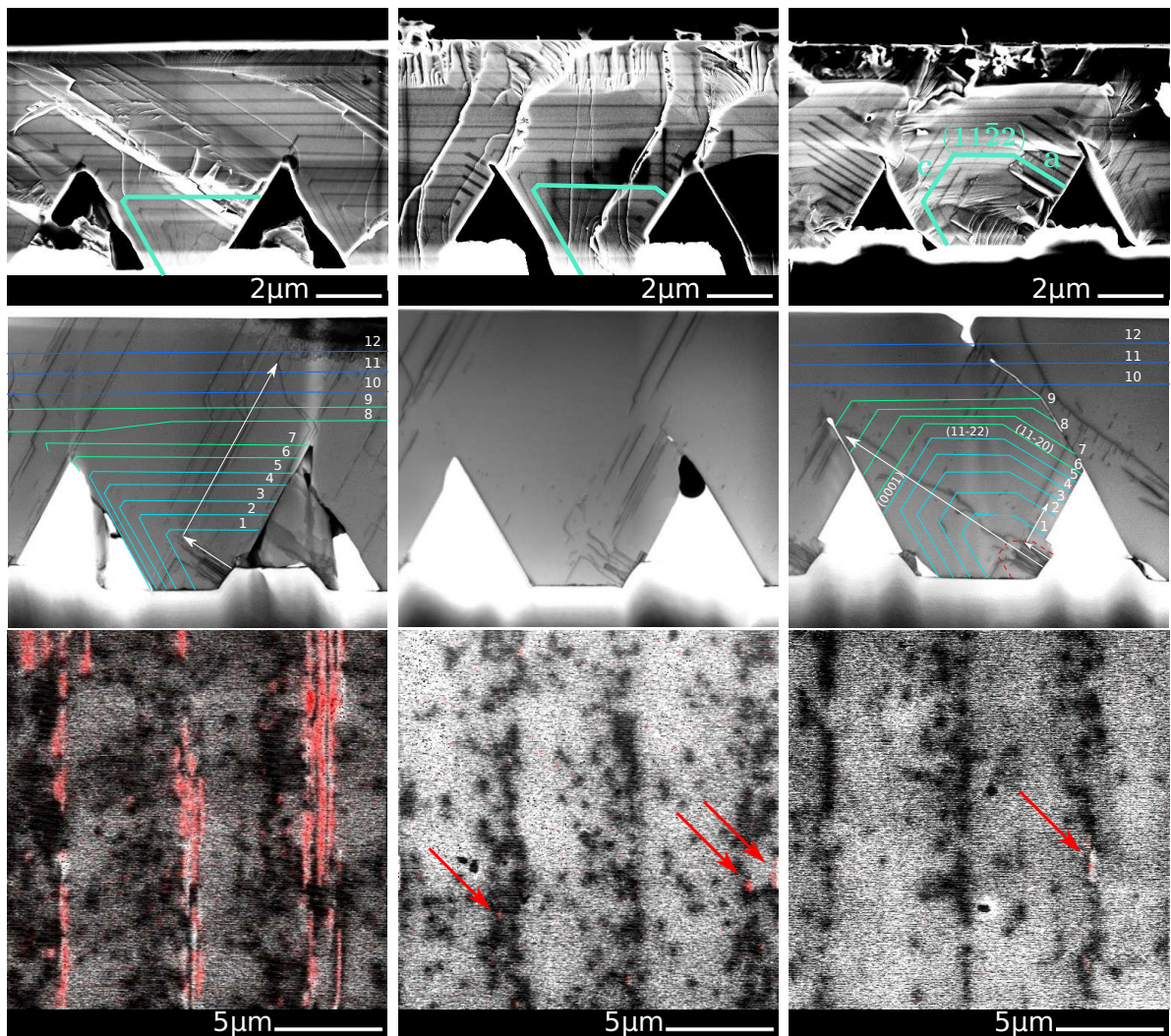


Fig. 2: Samples A (left), B (center), and C (right). First row: SEM cross-section. Second row: TEM images correlated with the course of the marker layers detected by SEM. The white arrows indicate the course of TDs. As soon as a TD hits the $(11\bar{2}2)$ plane, it bends from the c- into the a-direction. The red dashed line indicates the estimated course of the SiN_x interlayer. Third row: Low temperature CL measurement (3 keV, $T = 10$ K) of the wafer surface. The images are a superposition of a panchromatic map (grayscale) and the luminescence of the BSF I_1 (red).

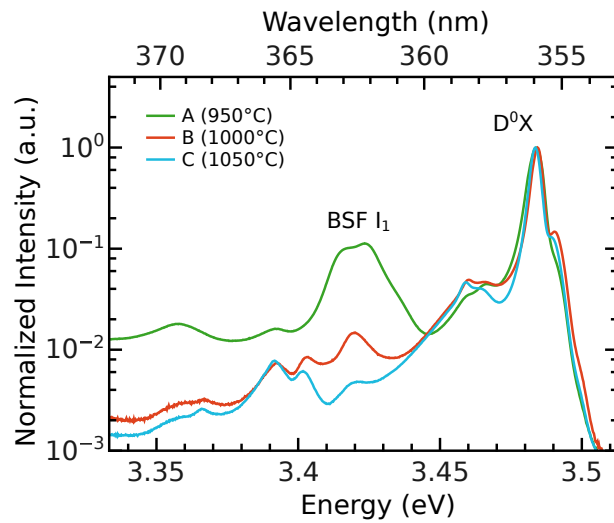


Fig. 3: Low temperature PL spectra measured at $T = 15\text{K}$ for the samples A–C. Due to the coalescence gap, BSFs are most effectively blocked in sample C, while sample A shows the highest density of BSFs on the surface.

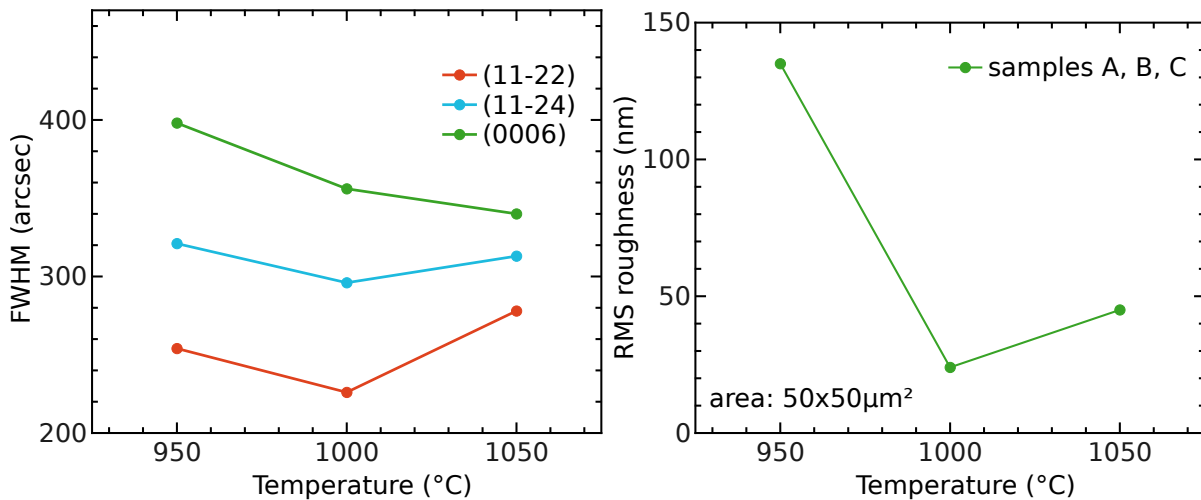


Fig. 4: HRXRD and AFM results. The temperature indicates the growth temperature before coalescence of samples A, B, and C. Sample B is clearly the optimum.

The TEM micrographs also confirm that sample B is the best (Fig. 2, second row). For both samples A and B, the c-plane is (almost) not existent. Thus, the dislocations bend early. However, in sample B many dislocations can be blocked by the gap at the coalescence point. In sample A, all dislocations can propagate to the surface, which might be the worst case scenario. Sample C has a huge c-plane facet just before coalescence. Therefore, dislocations might never bend. However, if the coalescence gap is big enough, they can be blocked (Fig. 2, second row, right).

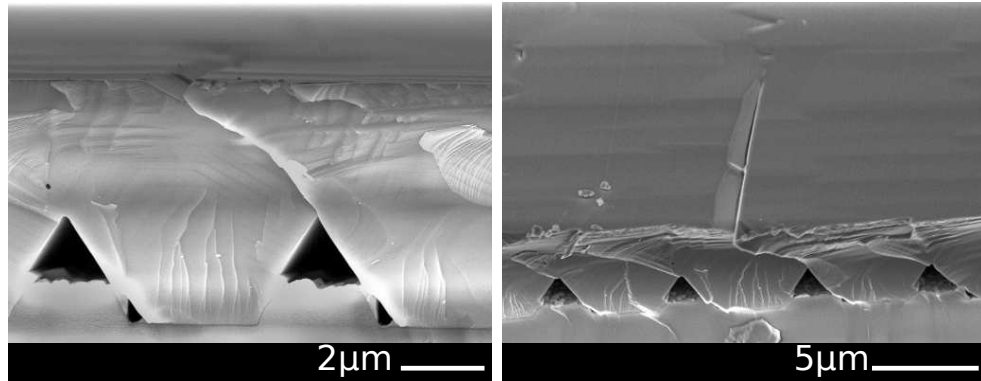


Fig. 5: Cross-section of failed coalescence leading to a “V”-pit (left). Bird’s eye view of “V”-pit (right). SEM images of a fissure resulting in a “V”-pit on the surface of sample C.

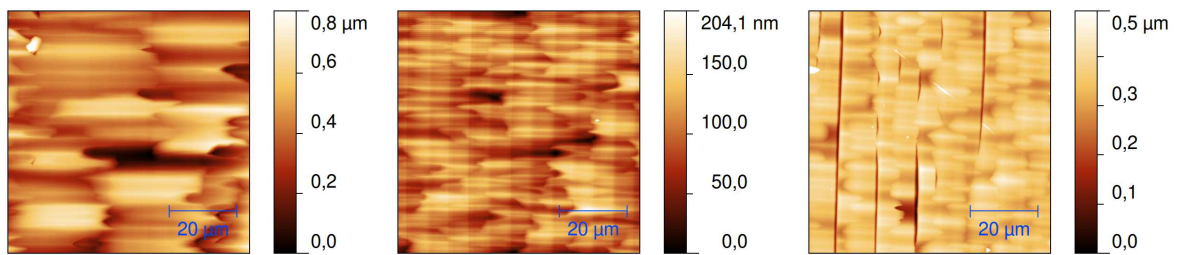


Fig. 6: AFM images of samples A, B, and C. The sapphire trenches are oriented vertically.

3.3 CL investigations

The low temperature cathodoluminescence (CL) measurement results of the wafer surface (3 keV, $T = 10$ K) are consistent with the findings of TEM. In Fig. 2 (bottom row), the superposition of the panchromatic map (gray scale) and BSF I_1 intensity (red) is depicted. Sample A shows the highest density of dark spots and BSFs, because both the TDs and SFs can propagate unhindered to the surface. Sample B has a clearly reduced density of dark spots and BSFs. We find that the dark spots are clustered in lines, while the BSFs are mainly aligned on the -c side parallel to the dark spots. Consistent with the PL measurement (Fig. 3), almost no BSFs can be found on sample C. Because of the huge gaps and fissures, also a lot of the dislocations can’t propagate to the surface resulting in an even smaller dark spot density compared to sample B.

Due to the superposition of the dark spots, it is not possible to determine their density exactly. The dark spot density could only be estimated roughly to $3 \cdot 10^8 \text{cm}^{-2}$, $1 \cdot 10^8 \text{cm}^{-2}$ and $8 \cdot 10^7 \text{cm}^{-2}$ for the samples A, B, and C, respectively.

4. Conclusion

In this study layers of $(11\bar{2}2)$ oriented GaN were grown on pre-structured sapphire substrates. We found that a variation of the shape of the initial GaN stripes has a huge impact on the coalescence behavior and the resulting layer and surface quality. We observed that threading dislocations starting from the stripe-shaped, c -oriented sapphire GaN interface in c -direction are bent by 90° as soon as they hit the $(11\bar{2}2)$ plane. In GaN stripes with a comparably large c -plane facet, TDs might never bend and continue up to the wafer surface.

We conclude that we have to make a compromise between a minimum TD density, a minimum BSF density, a good coalescence, and a smooth surface. Thus, an intermediate growth temperature of 1000°C of the initial GaN stripes before coalescence seems to be the best choice. Higher growth temperature of the initial GaN stripes would lead to smaller BSF density, but then a c -plane emerges, preventing TDs from bending into the a -plane and continuing unhindered to the wafer surface. In contrast, at lower growth temperature, BSFs from the $-c$ -wing propagate to the wafer surface resulting in a large BSF density.

Acknowledgment

I thank the co-authors of the full version of this article [1], namely Y. Han and C. Humphreys of the Department of Materials Science and Metallurgy of the University of Cambridge, United Kingdom, for TEM measurements, M. Hocker and K. Thonke of the Institute of Quantum Matter, Semiconductor Physics Group at Ulm University, Germany, for CL measurements, as well as T. Meisch and F. Scholz of the Institute of Optoelectronics at Ulm University, Germany, for scientific support. For technical support in the structuring of the sapphire wafers, I thank R. Rösch and C. Steinmann of the Institute of Optoelectronics at Ulm University. This work was financially supported by the European Commission (FP7) within the framework of the project “AlGaInN materials on semi-polar templates for yellow emission in solid state lighting applications” (ALIGHT).

References

- [1] M. Caliebe, Y. Han, M. Hocker, T. Meisch, C. Humphreys, K. Thonke, and F. Scholz, “Growth and coalescence studies of $(11\bar{2}2)$ oriented GaN on pre-structured sapphire substrates using marker layers”, *Phys. Status Solidi B*, vol. 253, pp. 46–53, 2016.
- [2] F. Scholz, T. Wunderer, B. Neubert, F. Feneberg, and K. Thonke, “GaN-based light-emitting diodes on selectively grown semipolar crystal facets”, *MRS Bulletin*, vol. 34, pp. 328–333, 2009.
- [3] T. Takeuchi, H. Amano, and I. Akasaki, “Theoretical study of orientation dependence of piezoelectric effects in wurtzite strained GaInN/GaN heterostructures and quantum wells”, *Jpn. J. Appl. Phys.*, vol. 39, pp. 413–416, 2000.

-
- [4] F. Bernardini, V. Fiorentini, and D. Vanderbilt, “Spontaneous polarization and piezoelectric constants of III-V nitrides”, *Phys. Rev. B*, vol. 56, pp. R10024–R10027, 1997.
- [5] O. Ambacher, “Growth and applications of group III-nitrides”, *J. Phys. D: Appl. Phys.*, vol. 31, pp. 2653–2710, 1998.
- [6] A.E. Romanov, T.J. Baker, S. Nakamura, and J.S. Speck, “Strain-induced polarization in wurtzite III-nitride semipolar layers”, *J. Appl. Phys.*, vol. 100, pp. 023522-1–10, 2006.
- [7] N. Okada, A. Kurisu, K. Murakami, and K. Tadatomo, “Growth of semipolar (11 $\bar{2}2$) GaN layer by controlling anisotropic growth rates in r-plane patterned sapphire substrate”, *Appl. Phys. Express*, vol. 2, pp. 091001-1–3, 2009.
- [8] P. de Mierry, N. Kriouche, M. Nemoz, S. Chenot, and G. Nataf, “Semipolar GaN films on patterned r-plane sapphire obtained by wet chemical etching”, *Appl. Phys. Lett.*, vol. 96, pp. 231918-1–3, 2010.
- [9] A. Kurisu, K. Murakami, Y. Abe, N. Okada, and K. Tadatomo, “Characterization of semipolar (11 $\bar{2}2$) GaN on c-plane sapphire sidewall of patterned r-plane sapphire substrate without SiO₂ mask”, *Phys. Status Solidi C*, vol. 7, pp. 2059–2062, 2010.
- [10] F. Habel, P. Brückner, and F. Scholz, “Marker layers for the development of a multistep GaN FACELO process”, *J. Cryst. Growth*, vol. 272, pp. 515–519, 2004.
- [11] J. Hertkorn, P. Brückner, S.B. Thapa, T. Wunderer, F. Scholz, M. Feneberg, K. Thonke, R. Sauer, M. Beer, and J. Zweck, “Optimization of nucleation and buffer layer growth for improved GaN quality”, *J. Cryst. Growth*, vol. 308, pp. 30–36, 2007.
- [12] J. Bläsing, A. Krost, J. Hertkorn, F. Scholz, L. Kirste, A. Chuvilin, and U. Kaiser, “Oxygen induced strain field homogenization in AlN nucleation layers and its impact on GaN grown by metal organic vapor phase epitaxy on sapphire: An X-ray diffraction study”, *J. Appl. Phys.*, vol. 105, pp. 033504-1–9, 2009.
- [13] M. Caliebe, T. Meisch, B. Neuschl, S. Bauer, J. Helbing, D. Beck, K. Thonke, M. Klein, D. Heinz, and F. Scholz, “Improvements of MOVPE grown (11 $\bar{2}2$) oriented GaN on prestructured sapphire substrates using a SiN_x interlayer and HVPE overgrowth”, *Phys. Status Solidi C*, vol. 11, pp. 525–529, 2014.
- [14] M. Caliebe, T. Meisch, M. Madel, and F. Scholz, “Effects of miscut of prestructured sapphire substrates and MOVPE growth conditions on (11 $\bar{2}2$) oriented GaN”, *J. Cryst. Growth*, vol. 414, pp. 100–104, 2015.
- [15] B. Lacroix, M.P. Chauvat, P. Ruterana, G. Nataf, and P. De Mierry, “Efficient blocking of planar defects by prismatic stacking faults in semipolar (11 $\bar{2}2$)-GaN layers on m-sapphire by epitaxial lateral overgrowth”, *Appl. Phys. Lett.*, vol. 98, pp. 121916-1–3, 2011.

- [16] N. Kriouche, M. Leroux, P. Vennéguès, M. Nemoz, G. Nataf, and P. de Mierry, “Filtering of defects in semipolar (11 $\bar{2}2$) GaN using 2-steps lateral epitaxial overgrowth”, *Nanoscale Res. Lett.*, vol. 5, pp. 1878–1881, 2010.
- [17] F. Tendille, P. De Mierry, P. Vennéguès, S. Chenot, and M. Teisseire, “Defect reduction method in (11-22) semipolar GaN grown on patterned sapphire substrate by MOCVD: Toward heteroepitaxial semipolar GaN free of basal stacking faults”, *J. Cryst. Growth*, vol. 404, pp. 177–183, 2014.
- [18] S. Schwaiger, S. Metzner, T. Wunderer, I. Argut, J. Thalmair, F. Lipski, M. Wieneke, J. Bläsing, F. Bertram, J. Zweck, A. Krost, J. Christen, and F. Scholz, “Growth and coalescence behavior of semipolar (11 $\bar{2}2$) GaN on pre-structured r-plane sapphire substrates”, *Phys. Status Solidi B*, vol. 248, pp. 588–593, 2011.
- [19] F. Brunner, F. Edokam, U. Zeimer, W. John, D. Prasai, O. Krüger, and M. Weyers, “Semi-polar (11 $\bar{2}2$)-GaN templates grown on 100 μ m trench-patterned r-plane sapphire”, *Phys. Status Solidi B*, vol. 252, pp. 1189–1194, 2015.
- [20] T. Zhu, C.F. Johnston, M.J. Kappers, and R.A. Oliver, “Microstructural, optical, and electrical characterization of semipolar (11 $\bar{2}2$) gallium nitride grown by epitaxial lateral overgrowth”, *J. Appl. Phys.*, vol. 108, pp. 083521-1–8, 2010.
- [21] L.J. van der Pauw, “A method of measuring the resistivity and Hall coefficient on lamellae of arbitrary shape”, *Philips Technical Review*, vol. 20, pp. 220–224, 1958.
- [22] K. Hiramatsu, K. Nishiyama, M. Onishi, H. Mizutani, M. Narukawa, A. Motogaito, H. Miyake, Y. Iyechika, and T. Maeda, “Fabrication and characterization of low defect density GaN using facet-controlled epitaxial lateral overgrowth (FACELO)”, *J. Cryst. Growth*, vol. 221, pp. 316–326, 2000.
- [23] P. Vennéguès, B. Beaumont, V. Bousquet, M. Vaille, and P. Gibart, “Reduction mechanisms for defect densities in GaN using one- or two-step epitaxial lateral overgrowth methods”, *J. Appl. Phys.*, vol. 87, pp. 4175–4181, 2000.
- [24] V. Wagner, O. Parillaud, H.J. Bühlmann, M. Ilegems, S. Gradecak, P. Stadelmann, T. Riemann, and J. Christen, “Influence of the carrier gas composition on morphology, dislocations, and microscopic luminescence properties of selectively grown GaN by hydride vapor phase epitaxy”, *J. Appl. Phys.*, vol. 92, pp. 1307–1316, 2002.